Automated Assessment and Tracking of Human Body Thermal variations using unsupervised clustering

Bardia Yousefi, Julien Fleuret, Hai Zhang, Xavier P.V. Maldague

Department of Electrical and Computer Engineering, Laval University, Qubec, QC G1V 0A6, Canada

Raymond Watt

RT Thermal company, 7167 Elkhorn Dr., West Palm Beach, FL. 33411 USA

Matthieu Klein

Visiooimage Inc., 2560, Rue Lapointe, Sainte-Foy, G1W 1A8, Quebec City, Canada

Abstract

The presented approach addresses a review on the overheating which occurs during radiological examinations such as MRI and a series of thermal experiments to determine the thermal suitable fabric material which should be used for radiological gowns. Moreover, an automatic system for detecting and tracking of the thermal fluctuation is presented. It applies HSV based kernelled k-means clustering which initializes and controls the points which lie on the Region of Interest (ROI) boundary. Afterwards a particle filter tracks the targeted ROI during the video sequence independent to previous locations of the overheating spots. The proposed approach was tested during some experiments and under conditions very similar to those used during real radiology exams. Six subjects have voluntarily participated in these experiments. To simulate the hot spots occurring during the radiology, a controllable heat source was utilized near the subjects body. The results indicate promising accuracy for the proposed approach to track the hot spots. Some approximations were used regarding the

*Bardia Yousefi, Xavier P.V. Maldague

Email address: bardia.yousefi@ieee.org and Xavier.Maldague@gel.ulaval.ca. Tel: (+1)418-656-2962 (Bardia Yousefi, Julien Fleuret, Hai Zhang., Xavier P.V. Maldague)

transmittance of the atmosphere and emissivity of the fabric could be neglected because of the independency of the proposed approach for these parameters. The approach can track the heating spots continuously and correctly, even for moving subjects, and provides considerable robustness against motion artifact, which usually occurs during most medical radiology procedures.

Keywords: Thermal image analysis, HSV unsupervised clustering, hot spot detection, particle filter tracking.

---

1. Introduction

. The measurement of body temperature using non-invasive methods is a challenging task which involves many researchers in the thermography field itself. Thermal instruments provide a powerful tool to avoid the invasive operations which are inconvenient or uncomfortable for human subject. During radiological exposure, any external tools could cause artifacts in radiology images and the procedure itself may represent a risk for the health of the patients. The medical applications of thermography have recently expanded [1] and involve various fields of medicine such as breast cancer [2, 3], dermatology [4, 5], avian flu [6, 7], dentistry [8, 9], psychology [10], and prevention.

Here the applications of thermography focus on medical prevention of burning during a radiological examination. The sudden death of the infant syndrome has been analyzed through the observation of the facial temperature increasing [11, 12]. In most of the applications the image filtering is manually done or analyzed by examining the images in the long intervals [13]. Moreover, it might be the essential to track the temperature due to the stationary location of the subject during the acquisition [14] and the markers may not be required for aid in tracking the body [15]. The current approach is motivated from a research study on epilepsy [16] which tracks the body temperature for thermal monitoring. The corresponding temperature attained by the averaging of pixel values from given images of the thermal camera was tracked during the examination. The temperature in the field of view (FOV) might have slight changes over time

in the video sequences, and is highly influenced while the subject is wearing the radiological gown or cloth. An active contour can include the specified region which comprises the area of the human patient and the possible heated spots on the mentioned region. However, a particle filter can track these spots for any increases in the temperature.

This investigation began with a short review on burning and dermatological effects described in next section. Afterward, an investigation to find a suitable radiology gown which can give a better thermal response (transmissivity) is described. Finally, a thermal image processing techniques for finding and monitoring the thermal spots within the increasing temperature is provided. It involves the authors as human subjects at the early version of this work [17] in the experiments involving a comfort test and thermal spot detection.

2. Problem Statement

Magnetic Resonance Imaging (MRI) is a medical radiology imaging system used to visualize internal structures of the body. A MRI scanner is a device in which the patient lies within a large, powerful magnet where the magnetic field is used to align the magnetization of some atomic nuclei in the body, and radio frequency magnetic fields are applied to systematically alter the alignment of this magnetization. This causes the nuclei to produce a rotating magnetic field detectable by the scanner - and this information is recorded to construct an image of the scanned area of the body. MRI provides good contrast between the different soft tissues of the body which makes it useful particularly in imaging of the brain, muscles, the heart, and cancers compared with other medical imaging techniques such as computed tomography (CT) or X-rays. Unlike CT scans or traditional X-rays, MRI does not use ionizing radiation. MRI is a technique of medical radiology which is painless and avoids exposure to X-ray radiation. MRI scanning involves no side effects for the human body. There is, however, the issue of patients who have metallic materials in their body. Metallic materials, chips, foreign materials (i.e. prosthetic devices, artificial joints

and metallic bone plates, pacemakers, etc) and surgical clips can significantly influence the MRI image. Moreover, metal implants and heart pacemakers or metal clips in or even around the eyes of patients cannot be scanned through MRI due to the movement of metal objects in the magnetic field. This includes metallic ear implants, artificial heart valves, bullet fragments, insulin pumps and even chemotherapy patients. Also, the claustrophobic sensation inside the magnet coil of the MRI scanner would be uncomfortable for claustrophobic patients. There are some cases of joint pain (hip joint) and tenderness, rib cage pain from fibrosing disease called Nephrogenic (Nephrogenic Systemic Fibrosis (NSF)). Several MRI patients have reported serious skin, muscle contracture, tightening, swelling and stiffness.

Some problems could occur since the radiology instruments (e.g. MRI) are normally tuned for higher SAR so that when lower SAR scans are conducted, the energy level could be too high which causes over-heating. For now, no procedure exists that enables the early detection of such body heating. The difficulty arises in the fact that the patients body is covered by a gown so there is no direct access to the skin to allow body temperature to be measured. Moreover, it is not possible to insert a probe since all metal is prohibited on the scanned body during the scan. These difficulties cannot overshadow the importance of radiology and medical imaging these instruments in medical diagnosis, their minimal side-effects and precise accuracy (particularly for MRI). On the other hand, the over-heating issue is clearly not acceptable under any circumstances. The objective of this research is monitoring and assessing the overheating spots using thermography images from the human subject during the radiology examination. This will help to prevent any kind of burning sensation for patients and assist the radiologist in his duty.

3. Effects of MRI

Man-made and natural ionizing or non-ionizing radiations sources i.e. Electric and Magnetic Field (EMF) are known to influence human life. One particular source of electromagnetic radiation affecting humans is the radiation medical examinations. In 1987, the radiation in medical examinations was above the natural amount, however this has changed since then [18, 19]. Diagnosis examination machine in the radiology, such as MRI, have became a significant reason of EMF pollution and the number of people who are under MRI exposure has dramatically increased. The risk that electromagnetic and ionizing radiation exposure represents for the environment and human health is not well documented and its effects for patient safety are not clear. Also due to the essential advantages of MRI, this procedure has became much more common and in the biomedical area. Nowadays, the number of MRI machines available in clinics has increased significantly and its utilization is highly recommended compared to the high radiation exposure radiology machines such as X-ray and positron Emission Tomography (PET). The genotoxic effects of MRI have been presented for the first time by Simi et al. (2008) from a micronuclei (MN) induction perspective. There is an association with MN frequency by early carcinogenesis events which is mentioned in the preliminary results [20]. There is no full confirmation for health hazard factor from MRI. Also there is very shaded information regarding genetic/biological effects and implication of health suggested via division of two cells enough to eliminate lymphocyte MN may occur. Three kinds of different fields have been considered namely radiofrequency (RF), gradient MF and static MF and their effects have been considered regarding the occupational risk and safety of patients [21, 22, 23, 24]. Patient burning and focal heating have been reported during clinical investigations utilizing MRI [25, 26, 27, 28]. These injuries mainly took place while there was a connection to some sort of device for physiological monitoring with skin contact by cable or monitoring sensors [29, 30, 31, 32, 33]. In addition, there were some reports regarding hypersensitivity to EMF exposure for extended time periods however the lit-

erature in this respect is still inadequate. Dermatological syndrome symptoms are mentioned in literature including some objective symptoms (dryness and redness) and mainly subjective symptoms (burning, and itching) due to EMF exposure. However, this investigation includes video display units but there is a link among these devices [34]. In general, radio frequency (100 kHz-300GHz) which is mainly applications in the mobile communication devices as well. To measure the signal exposure on humans, they have defined a score which is called Specific Absorption Rates (SAR), in watts per kilogram (W/kg). For instance, this value should not be above 2 W/kg for the human head according to the International Commission on radiation of Non-ionizing protection (ICNIRP) [35]. The medical application of RF electromagnetic fields for diagnosis and therapeutic purposes in this category has two groups of applications. The first group applies for healing the soft tissues, heating the tissues and treatment of cancer through hyperthermia [36] and the second group (MR included) involves uses for generating the MR signal [37]. Three kinds of MF have been used within MRI tests which produce three dimensional images [37].

1. High static MF for human body net magnetization;

2. A gradient MF (100-1000Hz) allowing spatial reconstruction of tissue sections into images;

3. RF electromagnetic wave (10 to 400 MHz) which energizes the magnetization vector and its detection by MRI scanner ad its conversion into MR images.

Various contrast levels follow the different physical and magnetic properties of biological tissues [37]. The highest risk is reported for patients using mechanical devices such as prosthetic and biomedical implants due to movements and rotational forces reasoned with the static field considering the distance and mass size [24, 37]. The risks associated with the use of MRI machines came to light following a tragic accident reported which led to the death of a six years old boy following on MRIscan, crushing the childs head when a metal oxygen tank sped across the room, pulled by the strong magnet [38]. The thermal injury accidents typically took place and were reported wherever there was a contact with a cable and monitoring sensor [39, 40]. MRI scanning of the cardiovascular

system involves potential hazards because of the existence of cardiac implants and devices (i.e. aortic stent grafts, coronary artery stents, implantable and pacemakers, cardioverter-defribrillators, and heart valve prostheses). The potential problems include possible dislodgement, dysfunction or movement of the cardiac device in the MF field [41]. MRI is considered to be a safe technology for medical imaging and radiology applications since it has an ability to change the atoms position without changing the composition and its properties which ionizing radiations tend to do. In any safe interventions, there are inherent hazards which must be considered. The aforementioned hazards can affect staff, patients and any other persons in the MR environment [42, 43]. To estimate the biological and dangerous effects linked with the MRI environment, many studies have been carried over the past thirty years which have produced many controversial results. These studies are related to biological consequences of a particular electromagnetic source during MRI. The recent findings for interactions between the biological system and MRI (EMF) should be.

3.1. Burning

Electromagnetic exposed to the patients considering time of this influence especially inducing through absorption of multi-photon in straight exposure [44]. The biological effects of exposure can be categorized in two groups: - Non-thermal effects: interaction of tissues and MFs directly; - Thermal effects: via tissue heating through electric currents induction; The studies on these effects principally occur from direct transfer of energy from the living system and depend on the field of frequency [41]. The absorption of RF energy increases the temperature of the tissues. The extent of temperature increase depend on many parameters such as geometrical and electrical characteristics, time and radiation frequency. One must note that the frequency of MRI scanning is tuned for high absorption in the patient body [35]. Some parts of human body are more sensitive to heating since they do not have perfusions, and consequently the existence of hot spots could be hazardous for the safety of patients [45, 46]. Furthermore, permanent cosmetics and tattoos on the skin with metallic

pigments (i.e. iron oxide) may reacts or have adverse effects which could cause first or second degree burns on the body [47, 48, 49]. Dosimetric parameters are usually employed as a standard of safety especially in absorption (using SAR) [50]. It is not easy to measure the energy of on MR scanner during its functioning so SAR represents a suitable factor for probable temperature increases. In general, the MRI scanning machine tunes to the correct information of the patients body (i.e. SAR). This amount has always been monitored and must not be above the standard limits which can be monitored by means of a scanning machine. If this value crosses the limit threshold of MRI scanning radiation, the scanning will be terminated automatically [50]. The recommended amount of SAR for the whole body is 4 W/kg, which is approximately equivalent to an increase in scanning temperature of $0.6°C$ for 20-30 minutes of scanning time [51, 52]. If this recommendation is respected no hot spot will occur and the SAR of the entire human body will be safely under the threshold limit [53, 54].

3.2. Analysis of vitro effects

Radiofrequency exposure and mammalian body cell genotoxicity, toxicity, and transformation has been reviewed in the literature for the vitro situation (because of the cellular telecommunication telephones high RF field (900-1100 MHz)) [55]. It is noticeable that the energy which radiates from mobile telephones is less to break bonds among the molecules and chemical bonds, whereas there are some reports regarding aberrations of chromosomes, induction of micronuclei in fibroblasts and DNA strand breaks [56] plus strand breaks in DNA of embryonic stem cells due to increasing in the transient [57]. Some experiments tried to evaluate the influences on the exposure of RFs into the micronuclei and proliferation of cells for cultural peripheral blood lymphocytes, however no evidence regarding tcytotoxicity and genotoxicity has been found [58]. Few studies have been conducted on the influences of RF frequencies on MR processes. However, the entire data analyzed on the mammalian cell cultures presents no cause for any kind of genetic mutation or frequency aberration of chromosomes (or frequencies exchange in sister chromatids) and the results mentioned that it

is improbable that MR exposure be genotoxic [24, 59]. Some reasonable consistencies for endpoints in biological systems are attained in the treatment of lymohocytes in humans [24]. This excludes thermal effects in the study [22] by changing the temperature of the flask of liquid in the exposure which was constantly below $1°C$ which is below the risk level [60].

3.3. Analysis of vivo and ex vivo effects

3.3.1. Mammals

Animal experimental studies were performed for reactions of thermoregulation in the heating of tissues through MR frequencies. However, the body temperature increased during the MR exposure within the experiment [41]. Due to the difference in anatomical feature structures, biology, sensitivity of tissues and body size, the results obtained for the absorption of RF in experiments conducted on animals cannot be extrapolated for the human body [43].

3.3.2. Humans

In the vitro experimental situation, studies were conducted regarding the effects of RF exposure and the frequency to determine if there is any probable connection between cancer risk and RF exposure [24]. There are a few studies regarding hypersensitivity to electromagnetic radiation involving non specific symptoms which are self-reported (e.g. difficulties in concentration, fatigue and headache) which suggests that they are not relevant to the exposure of RF [61]. The first experiment which studied the thermal effects of magnetic resonance imaging on human was conducted in 1985 [62]. Each subject was exposed to 4 W/kg SAR and the temperature changed with the physiology parameters. The other studies involving volunteers have always variation in body temperature below $0.6°C$ and without any changes in blood flow, blood pressure and heart rate [63, 64]. Another, MR procedure study [65] involving an exposure of the whole body to 6 W/kg SAR included controlled skin temperature, blood pressure, saturated oxygen, heart rate and blood flow of skin. These parameters

changed in very acceptable range considering the safety level. The summarized evaluation of physiological effects for 2000 cases showed changes in the neural, endocrine, auditory, visual, immune, reproductive, developmental functions and cardiovascular in high stage of disclosure of RF [41]. Particularly over-heating in the eyes [45, 24] and gonads [64] via diminishing of the ability of dissipation of heat thus existence of the probable hot spots considering the mentioned temperature was within the safety limit. It has been mentioned that MRI procedures interact with biological tissues which could be hazardous for patients [**?**]. In addition, accidents of burning through creation of hot spots in the presence of materials located near the patient, i.e. equipment used for monitoring parameters of philological leads, have been reported. Especially the biomedical implants which are used internally or activated electrically are at risk during MR exposure.

The general cure modality regarding liver cancer is inoperable through radiofrequency (RF) ablation. Skin burning is of increasing concern due to increasing the capabilities of high power RF which creates larger ablation zones. The maximum temperature is due to the ablation zone which is determined by a MRI scanner [66] but no significant points regarding the burning issue have been mentioned. The effect of 8 Tesla MRI and its disadvantages which is related to influences of the electromagnetic radiation on the living tissues has been mentioned. This analysis presents a technique regarding the coil modification which can be a cause of control coil width (gauge) and depth of image. This control the affects of the electromagnetic on the skin during medical Micro-coil MRI scanning [67]. Burning of the skin under RF exposure ablation is more common; however the high power generator of RF is able to generate the ablation zone for tumor effects in new applications. The aim is to estimate the decrease in temperature of skin using additional ground pads to the vivo-porcine model. The analysis follows the normal procedure for three pads located in the abdomen of animals for thermal analysis. The experiment was exposure of thirteen RF carried out for 12 minutes by two internally cooled clusters. Degree of burning and rising in temperature inside the attached pads was determined under a T2-

weighted MRI scanner. The results of this method revealed that the estimated temperature of ground pads are lower than the temperature which would lead to skin burning [68].

Gayton et al. (2010) analyzed the surgical staples and removable suture materials on three pig-feet (five surgical staples repairs with 3-cm surgical incisions) in the exposure of 1.5 Telsa MRI scanning machine for 35 minutes. The analysis of skin temperature was measured along with the staple movement. Thermal changes were evaluated being $14.60°C$ to $18.20°C$ (STD=$0.70°C$) and no changes occurred in the position of the staple. Also the new structure of the medical lead for diminishing the scatter-field has been introduced. A considerable reduction of the electric-field has been observed which presented a solution for the problem of heating during MRI scanning and a reduction in effects for medical implants in various frequencies of MRI [69] and MRI effects on the surgical staples analyzed in [70]. The effects of the electric field at the cell level have been numerically analyzed in cell culture. Thermal increments measured during the exposure considering the $1°C$ thermal threshold led to common biological effects. However, after exposure to pulse-modulation imitating an ultrahigh field for MRI, the temperature increases did not trigger any threshold response.

3.3.3. 3D Analysis

For analysis of the human body temperature, a 3D thermal model of the body can be constructed during MRI exposure. By 3D analysis of the infrared image, the thermal 3D model of the body allows the overheating points to be detected. In this section, a brief review of 3D processing is presented. The human body is a living organism which has changes in internal factors and external form and is constantly in motion. These variations involve many factors such as pose shifts, fluid distributions in the body, sway, respiration and occlusion which create many limitations and difficulties in the topology of the body. Scattering properties, skin pigmentation and especially the radiology gown are considered as the limitations which create problems in accurate measurement.

The use of infrared images helps to overcome the mentioned difficulties however infrared images have their own limits and barriers. An explanation of the indoor thermal radiation environment in the human body has been analyzed through 3D modeling of the human body in some poses and situations [71].

A 3D X-ray microtomography image analysis of low density wood fiberboard has been done. It used for the prediction and modeling of local densification with material behaviour and similarity under radiation exposure. However, the type of radiation is different [72]. The study in 3D visualization of fiber is not limited to this investigation and has been studied in greater detail (for example [73]) which is not very relevant to topic. There is another application of 3D reconstruction using thermal images for detection of infection in the skin of patients. To avoid too much human body surface information which is not very possible, there is an integration of 3D high resolution far-infrared FIR thermal images and true color imaging of the body surface has been used for 3D structural binocular profilemeter [74]. The research on jet fuels toxicity concerning skin damage measured by 900MHz skin microscopy has been done. The authors applied three-dimensional spatial visualization that can show the skin structure and help draw conclusion regarding the toxicity [75].

Many medical image processing research studies have been done on 3D visualization of limbs and tissues under MRI scanning. The structural anatomy which has been considered by some 3D applications and registration can be summarized as including: vertebrae and Spin; Skull and brain (head); general, hip joint, femur, tibia, knee joint (limbs); perineum, entire (pelvis); heart, ribs, entire (thorax)[76]. Most of the research works on 3D (or even 2D) in biomedical image analyzing consider the area in: patient motion tracking, patient positioning (radiotherapy), arteriovenous malformation (radio-surgery) , embolization, shunt angioplasty (vascular interventional radiology), neck, head, and spine, procedures which are invasive (neuroradiology interventional), replacement of hip and knee, total arthroplasty hip (orthopedic surgery), knee kinematics (kinematic study) with the benefits for radiosurgery and radiotherapy applications [76]. However, the information covers many 3D medical applications and are

not considered as thermal applications. It gives valuable information regarding 3D (even 2D) analysis in medical image research. A 3D building construction using Infrared thermography images and real images has been presented [77] which is not categorized in medical image analysis but the idea is valuable in terms of the potential applications.

Applying an oriented scheme cubic for co-registration of the practical geometry of medical parts of the human body using points and 3-plane has been presented based on localization properties and fusion of MR, CT and PET images for creating a 3D model [68]. The model includes images fused across modalities of PET+MR, CT+MR, PET+CT, MR+CT+PET and has been tested on patients for detectability of tumors with considerable results. However, no thermal images or skin visualization was done. A very relevant research work regarding 3D surface thermal image construction has been conducted for energy auditing which gives a 3D surface temperature model [78]. This work is relevant however it was done for nonliving objects. Applying this technique for humans would make it a very useful system for relevant applications. Siewert et al. (2014) present a method for the analysis of body temperature in pige skinusing thermal infrared images. This approach has used the averaging value of the temperature for both ROI (from two anatomical regions in IR images) to overcome noise and its suppression [79].

4. Proposed method for automatic detection and tracking of hot spots

The problem of burning during MRI has been introduced and reviewed in the previous sections. This information leads to the possibility of using thermographic devices to create a system for the automatic detection and tracking of overheated spots during radiology within the thermal video sequence. The process should begin with on initialization and then control possible points which have overheated and which lie on the boundary of the ROI in every frame of the thermal video stream. To find the ROI during the video, two methods have been considered and will be explained in the coming sections below. The ROI

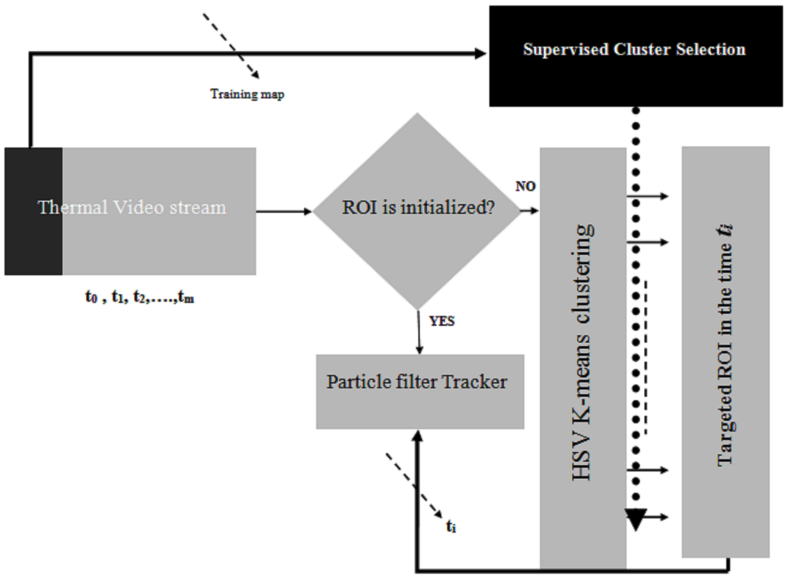

Figure 1: Here the flowchart of the proposed approach for automatic tracking of overheated regions.

is the initial step for the automatic particle filter tracker.

4.1. Active-contour and Region of Interest(ROI)

Detection of thermal changes is the first step of the process to find the ROI and high temperature in the thermal images. The process of finding the thermal increases is completed by conducting an active contour on the intensity (greyscale) thermal image. But before applying the active contour to select the ROI and provide the average of the intensity corresponding to the temperature of the area, the particular amount of intensity must be selected. The blackbody is used as a thermal reference in the entire experiments, to tune for the normal temperature of a healthy human body. Considering that the transmittance of the targeted object area and blackbody are the same, the intensity of both objects are very representative of the approximated temperature. The increment starts from the temperature of the blackbody and it increases within the time sequence. In every step of the sequence there is an update on the morphological

profile (MP) of the algorithm. MP contains many morphological operations such as dilating, eroding and filling operations which are used with the active contour and provide the ROI (ideally has a higher temperature). Intensity of this area can update initial intensity assumption and initiates the particle filter.

4.2. Unsupervised Clustering in HSV

Another approach, which can be used to determine the ROI and is seemingly more robust as compared with active contour, is the clustering of the thermal image obtained from the experiments. The main and first question which might be asked is why to use the Hue Saturation Value (HSV) for unsupervised clustering of the thermal image. The simple answer can be due to the separation of luma, which contains the intensity information of the image, from chroma which has the color information. It is more unlikely for the RGB color system which is normally used for the purposes of clustering. It is due to the reason that it gives the robustness of removing shadows or lighting variations. In the RGB color system, the implementation details regarding the color display are concerned, however in HSV the actual color components are in the target. Thus, RGB is more a computer treated way of the color to be shown and HSV is more look-like the capture of the components in the way that humans perceive the color. The response (or resonation) of the human eye is only limited to three main light frequencies and it is not surprisingly to red, green and blue, which is not linear. It provides pure color to distinguish the response of the retina combining three color component responses. Besides, the separation of luma and chroma provides a histogram construction or thresholding rules using only saturation and hue. This works regardless of lighting changes in the value channel and practical clustering gives reasonable efficiency. The unsupervised clustering method used for the purpose of the project is K-means clustering. It efficiently provides the ROI cluster from the thermal image which initiates the particle filter for tracking these regions in order to automatically detect and monitor the hot spots [80].

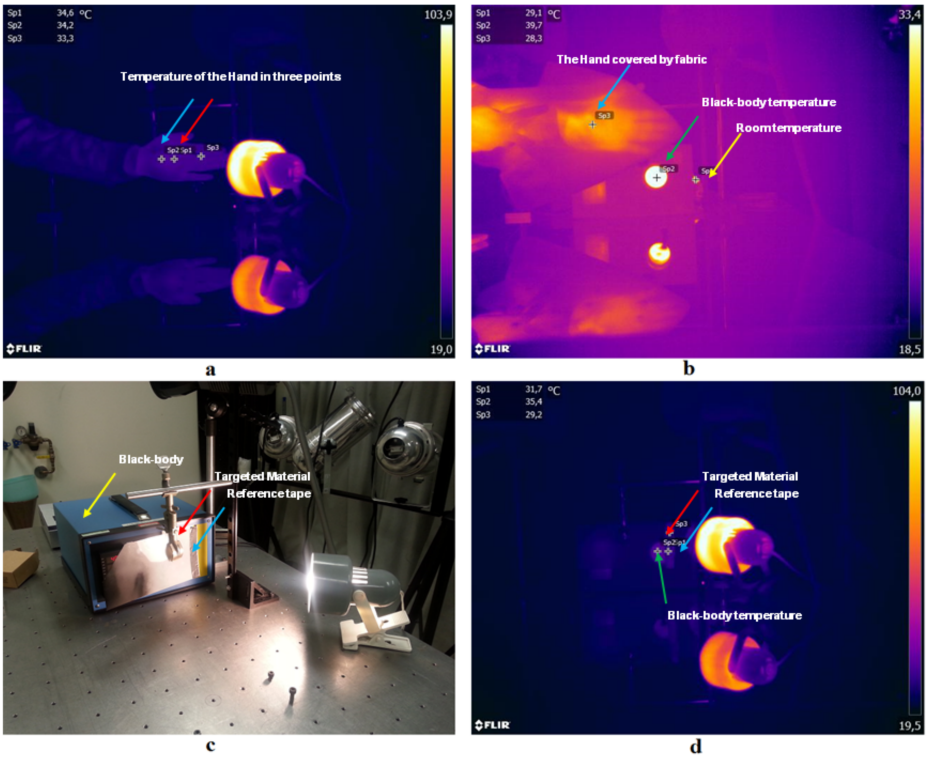

Figure 2: The temperature of the hand without being covered by fabric is shown at (a). The fabric was covered the hand(b). The black-tape and the table where the experiment was conducted(c). The blackbody was set for a particular temperature and the temperature before and after covering the blackbody with the targeted fabric (d).

4.3. Particle filter

The hotspot detection looks easier as compared with tracking the hot spots once the temperature updates and there is thermal expansion in the time. Tracking the hot spots involves chasing hot spots on the body surface and being confident that the ROI location will not be lost. A tracking algorithm needs to be reasonably robust since a surface is rarely uniform.

This approach uses a particle filter tracker [81] to track and adapt to the tracking task (particle tracking also used many times in medical image analysis for example [82, 83, 84]). It provides a robust system to face the changes in ROI

during the video sequences. The some assumptions considered for the tracking algorithm are as follows:

- The analysis of the thermal tracking takes place in the grayscale images from black to white having an intensity of 0 to 255 corresponding to the cold and hot range;

- The ROI is always in FOV of the thermal camera;

- Temperature of the ROI (subject) is higher than the surrounding environment;

- The temporary ROI does not have a particular shape and must to be adjusted through the algorithm. However the thermal increases (level of intensity) is an unpredictable contour shape having an upward trend. The unpredictable contour shape comprises the temporary occlusion and other unwilling external factors which influence the radiological images e.g. motion artifact;

- the ROI is updated during the experiment (radiological field exposure) and the temperature is updated by an upward trend to find the hot spots which are the cause of the burning in the subject.

Using a Bayesian method tracking algorithm, the particle filter works in the time t and approximates the tracking recursively of the target by a finite set of posterior distribution weighted samples. In general, particle filters are the simulation class filters for the approximation of random variables recursively. Let $\alpha_t|Y_t = (y_1, y_2, \ldots, y_t)$ are the random variables and $\alpha_t^1, \ldots, \alpha_t^M$ are particles having the discrete probability mass of $\pi_t^1, \ldots, \pi_t^M$. The discrete points approximation of the variables shown by $f(\alpha_t|Y_t)$ and for π_t^j are assumed to be equal to $1/M$ which is the desired amount of M for the particles to approximate the density of $\alpha_t|Y_t$. It is noticeable that the particles are located in the ROI which is previously defined and incrementally updates throughout the thermal experiment. The discrete support is used as the true density. It gives an approximation for the density prediction by particle support and empirical prediction:

$$\hat{f}(\alpha_{t+1}|Y_t) = \sum_{j=1}^{M} \hat{f}(\alpha_{t+1}|\alpha_t^j)\pi_t^j \tag{1}$$

A mixture of echoes whiles the filtering proceeds and density. This provides the following,

$$\hat{f}(\alpha_{t+1}|Y_{t+1}) \propto \hat{f}(y_{t+1}|\alpha_{t+1}) \sum_{j=1}^{M} \hat{f}(\alpha_{t+1}|\alpha_t^j)\pi_t^j \tag{2}$$

This is an approximation of the true density filtering. New particles produced $\alpha_{t+1}^1, \ldots, \alpha_{t+1}^M$ with weights $\pi_{t+1}^1, \ldots, \pi_{t+1}^M$ and this iterates through the data. This can include online tracking problems and an estimate of the one-step-ahead density $f(y_{t+1}|Y_t)$. It is relevant to updates of the ROI and the spreading of hot spots within the radiological exposure and is given in [80, 81].

5. Experimental and Simulation Results

This approach proposed a method for the detection of heating spots during the radiological examination using an infrared imaging system. The main part relates to computer system modification and simulation on image analysis. However, there is an important issue within involves selecting a suitable radiology gown that has a reasonable thermal property (particularly transmittance). The following section provides some information explained regarding the experiments conducted for some candidate fabric materials, experimental setup, and infrared image acquisitions. The results of proposed approach are then revealed by the analysis of the targeted fabric in the model situation for benchmarking. The experimental results reveal the effectiveness of the proposed method and relatively good property of the selected fabric.

5.1. Thermal properties of the fabric

Thermal properties of the fabric materials which are used as a gown during the test seem essential and need to be considered. There is extensive literature regarding different materials and their thermal properties such as emissivity and transmissivity. For instant, one of them presented by Ohman 1982, approached emissivity finding the sophisticated practical way by gathering the radiations of object, reflection and atmosphere [82].

$$\acute{S}_o = \epsilon_o \tau_o S_o + \tau_o(1-\epsilon_o)S_a + (1-\tau_o)S_{atm} \tag{3}$$

$$= object + reflected + atmosphere \tag{4}$$

Where ϵ_o, τ_o are emissivity and transmissivity of the object. To convert this relationship from radiation into thermal value, I, the S must be replaced with I/C that C is an empirical instrument factor [82].

$$\acute{I}_o = \epsilon_o \tau_o I_o + \tau_o(1-\epsilon_o) I_{ao} + (1-\tau_o) I_{atm} \tag{5}$$

$$\acute{I}_r = \epsilon_r \tau_r S_r + \tau_r(1-\epsilon_r) I_{ar} + (1-\tau_r) S_{atm} \tag{6}$$

Where I_{ao} and I_{ar} refer to the surroundings of the object and reference respectively. The thermal difference increase is measured by $\Delta i_{or} = \acute{I}_o - \acute{I}_r$ In a practical measurement situation, it is assumed that the object and reference are placed close together. Therefore $\tau_r = \tau_o = \tau$ and $I_{ao} = I_{ar} = I_a$ and the thermal values of the object considering the assumption is as follows [85]:

$$\epsilon_o = \frac{\Delta i_{or} + \epsilon_r \tau (I_r - I_a)}{\tau (I_o - I_a)} \tag{7}$$

The thermal values of the blackbody (calibration function at source temperature) are expressed by radiation terms. Depending on the instrument design and principle of measurement used in the actual situation the formula can be changed. Direct measurement has the great advantage that it does not require the reference. Here, a TEFLON taper has been used (as reference) but due to ease the calculation of the reference which has been eliminated and directed the measurement but considering all required approximations applied. Moreover, the transmittance estimation is the most important thermal parameter in this calculation (to evaluate the temperature of the patient body). The difference between the object real temperatures (in this case blackbody) and observed by a thermal camera is represented as the transmittance factor.

5.2. Experimental setup

The experiments were conducted in the normal room temperature. JENOPTIK-IR and FLIR cameras have been used for the infrared images acquisition due to

the similarity of JENOPTIK to FLIR at the wavelength ($7.5\mu m < \lambda < 13\mu m$) with the real experimental situation. A computer (CPU i7) has been used to gather the data from the camera. The possible fabric has been used based on the mentioned information for the calculation of the thermal properties. There is a possible fabric material considered as targeted in front of the IR camera. Behind the fabric the blackbody is located for particular temperature (normally around the body temperature). If the method follows the mentioned approach for the calculation, there will be a colour painted on the fabric or a TEFLON tape is used which is both representative of the known emissivity materials (reference in material). The experimental setup was arranged for convenience of estimation in the mentioned parameters. The most necessary property of thermal visibility of fabrics which is required for the radiology gown is the transmissivity and it is apparently essential to be taken into the account. Some temperature points are required for emissivity calculations using the described method shown in figure 3. For a quick and reasonable emissivity approximation, a suggestion involves placing the fabric on the top of the uniform temperature surface and measuring the temperature of spots before and after putting the fabric on the surface. It is essential to measure the temperature crossed from the fabric in equilibrium and stable temperature. This means that after placing the material on the top of the surface, the temperature must be uniformly distributed. It must be measured once the temperature of the fabric becomes stable. To calculate the transmissivity one proceeds the same way, but for transmissivity seeing thermally through the fabric is necessary. For the fabric transmissivity estimation, the temperature of the object without and with a fabric covering has been measured. For instant, shown in figure 2, the temperature of the hand with and without the fabric: $SP_1 = 34.6°C, SP_2 = 34.2°C, SP_3 = 33.3°C$. The average temperature of the hand is:

$$\frac{SP_1 + SP_2 + SP_3}{3} = \frac{34.6 + 34.2 + 33.3}{3} = 34.04°C \tag{8}$$

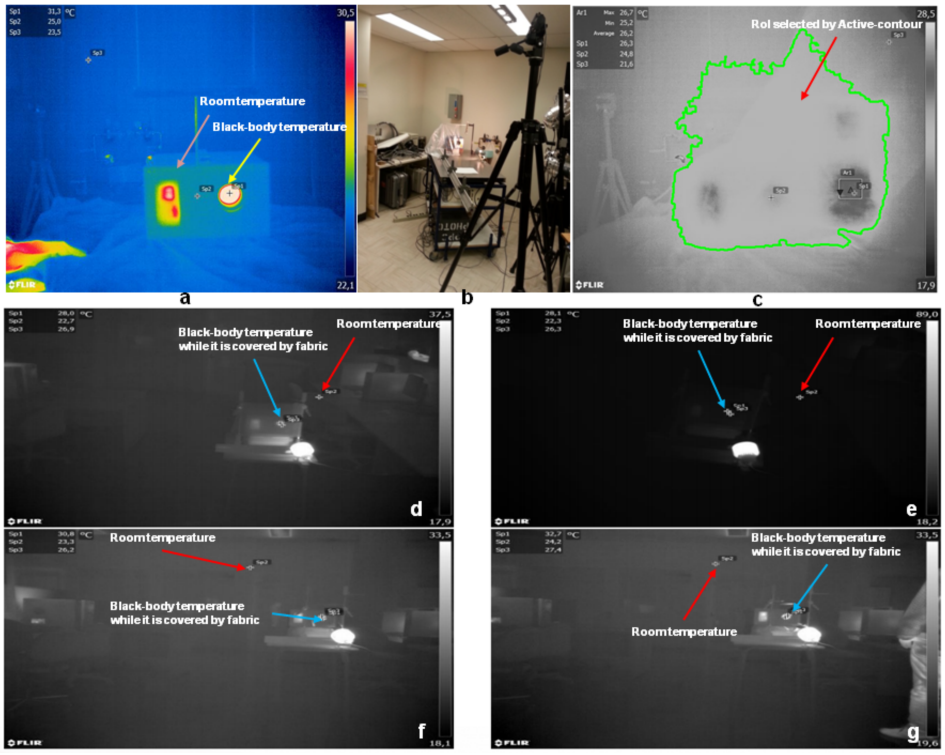

Figure 3: The experimental setup (b) of one of the several tests with some thermal images taken from transmissivity of the fabrics (a, d-g) and finding the ROI using the active contours(c) shown.

Then the temperature of the hand after being covered by the fabric which is shown by SP_3 in the second figure $SP_3 = 28.3°C$.

$$\tau = \frac{ObjectTemperatureAfterCoveringbyFabric}{ObjectTemperatureWithoutBeingCovered} \tag{9}$$

$$Transmissivity(\tau) = \frac{28.3}{34.04} = 0.83 \tag{10}$$

The 0.83 represents the fabric transmissivity which in this case is a denim fabric. To find a relatively suitable fabric, more than 40 different and possible fabrics have been tested to find better transmissivity for the application. Table 1 shows a list of the fabrics which have been tested to select a better choice of the fabric for the radiology gown. The camera was almost in front of the blackbody

Table 1: Table represents fabrics which have been tested.

Fabric number	Temperature before being covered	Temperature after being covered	Transmissivity of the fabric
1	313◦C	24.7◦C	0.789
2	313◦C	24.5◦C	0.783
3	313◦C	24.5◦C	0.783
4	313◦C	24.6◦C	0.786
5	313◦C	24.4◦C	0.779
6	313◦C	24.8◦C	0.792
7	313◦C	24.4◦C	0.779
8	313◦C	23.7◦C	0.757
9	313◦C	23.8◦C	0.7603
10	313◦C	24.0◦C	0.767
11	313◦C	24.7◦C	0.789
13	313◦C	24.6◦C	0.786
14	313◦C	24.5◦C	0.783
15	313◦C	27.0◦C	0.862
16	313◦C	26.4◦C	0.843
17	313◦C	26.1◦C	0.834
18	313◦C	25.5◦C	0.815
19	313◦C	25.3◦C	0.808
20	313◦C	24.6◦C	0.786
21	313◦C	25.0◦C	0.799
22	313◦C	28.3◦C	0.904
23	313◦C	25.2◦C	0.805
24	313◦C	25.0◦C	0.798
25	313◦C	24.6◦C	0.786
26	313◦C	24.5◦C	0.783
27	313◦C	25.2◦C	0.805
28	313◦C	24.9◦C	0.795
29	313◦C	24.9◦C	0.795
30	313◦C	24.9◦C	0.795
31	313◦C	24.6◦C	0.786
32	313◦C	25.0◦C	0.798
33	313◦C	24.8◦C	0.792
Targeted Fabric	313◦C	26.9◦C	0.85943

having on almost zero angle which provides a perpendicular situation for the test. However, all the calculations have been carried out, applying the analysis techniques in the normal situation experiment. But in general the transmissivity calculation in the perpendicular position provides a reasonable benchmarking criterion. As shown in figure 2, figure 3 and table 1, the temperature of the blackbody was $31.3°C$. This temperature was used in the calculation of the transmissivity. The calculation of the fabric transmittance is shown in Table 1.

5.3. Experiment on the hot spots tracking

The aforementioned analyses for finding the suitable fabric was done to find a suitable radiology gown. It provides more reliable thermal and machine vision properties to observe the hot spots and prevent possible burning during the examination. The procedure of the experiment was conducted to closely resemble the position of the patients during the radiology tests. The experiment was carried out on six participants (the participants were researchers and authors of the article [17]). The temperature was slightly lower than room temperature so go to more closely resemble the condition in an actual radiology room. Each participant wore the gown made with the selected fabric and lay down on the bed used for the experiment. The IR-camera is located in front of the bed and the distance of the camera and its angle was very similar to the actual situation in a radiology room. The duration of every experiment was approximately 11 minutes and JENOPTIK and FLIR cameras recorded the thermal variations. To simulate the hot spots in the human body, a controllable heating source was used. The heater temperature was set before the acquisition began to the targeted temperature which leads to a sensation of heat or burning. For this purpose, skin physiological information is needed that contains many parameters involved in the burning. However, for simplicity of the implementation the heat temperature has been chosen around $55°C$. The blackbody also has been utilized as a reference and has been set for the temperature of the human body in the normal situation. The blackbody was located next to the bed and in front of the IR camera (in the FOV). The controllable heater took several minutes to reach the required temperature and during this time all the thermal variations were recorded by IR-camera. The heater is located closed to the subject and the movements of the subject were minimal to resemble the real conditions as closely as possible. The experiment also involved the gown which is currently used for the radiology patients and which gives a lower thermal response (low transmissivity) as compared with the proposed gown. Figure 4 reveals the images of a subject during the experiment.

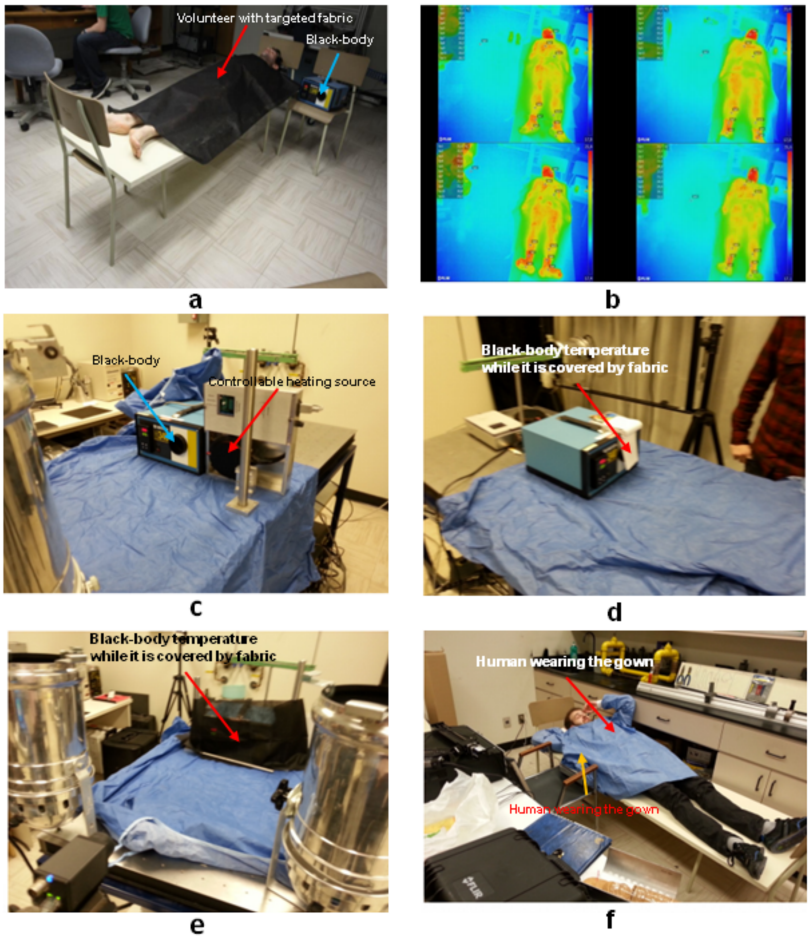

Figure 4: The experiments conducted for fabric transmissivity have been shown (c-f). The test for simulating the radiology test (a), thermal videos of the subjects shown in (b).

5.4. Results of the tracking

In this section, the results of the proposed tracking approach are presented. After solving the problem of the transmissivity of the gown, the proposed approach was applied to the real situation of the thermal video sequence to locate the hot spots. The k-means cluster was applied to find ROI which contains the human body region with a thermally higher intensity as a foreground, compared with the background with the lower temperature. As the k-means clustering is

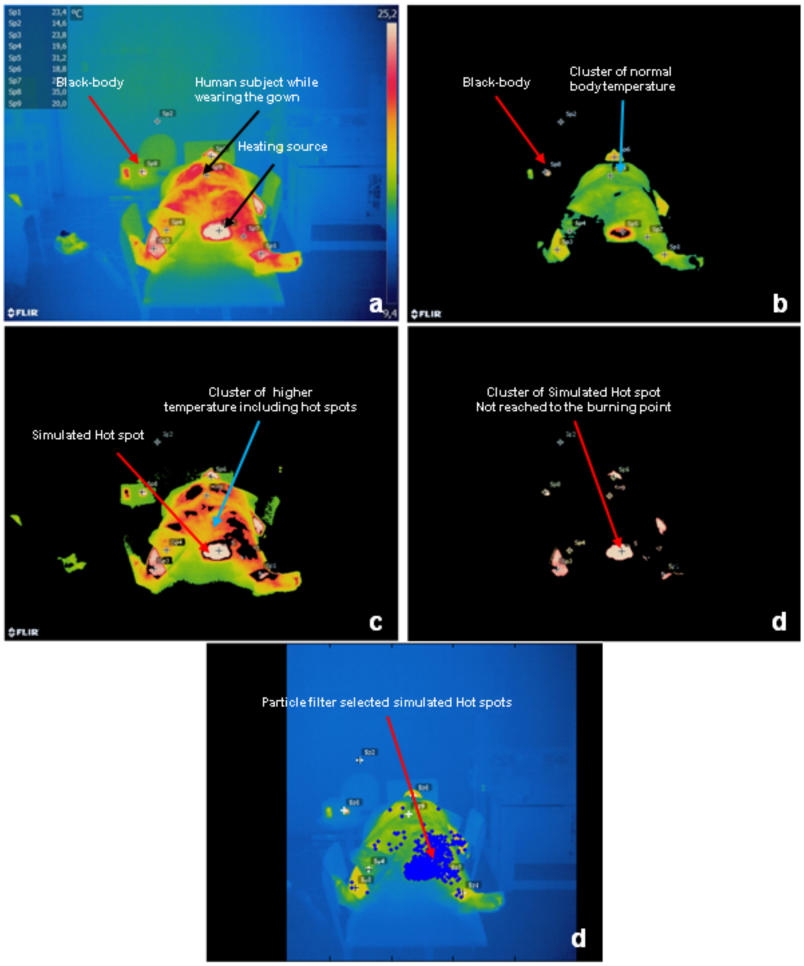

Figure 5: The results of the clustering for different clusters have been shown(b-d). The image at upper-left side reveals the original IR image taken with FLIR. The upper-right side and lower-left images show the human subject in different clusters. However, selecting the whole human body in the IR-image involves the system into several unnecessary morphological operations but it is a suitable technique for tracking the whole human subject. The lower-right side image represents the ROI to be tracked and monitored within the exposure of radiological beams(d). The last image reveals the particles while they are tracking the hot spots (d).

an unsupervised learning procedure, there was no training set used for the approach. The thermal video sequence was 30 frames per second which is high for the actual purpose of the approach. This is due to the slow process of the thermal variations during radiology examinations. Due to the mentioned fact and having the faster process of the purposed method, the system considered every second as one thermal frame processed. The sampling could be lesser, but applying the particle filter required stepwise variations to have a more efficient tracking. The size of thermal images for every frame included 560*640 pixels with a false color to improve the heat discrimination. The clustering provided the targeted ROI corresponding to the hot spots. These regions are given to the Particle filter for initiation and tracking within the test. The particle created for tracking the hot spots are spread throughout the human subject which gave possible points of over-heating. The particles concentrations represented the higher and more stable hot spots that were constantly tracked by the particles and provided the accurate detection within the thermal images. The other unstable hot points were not continuously tracked by the particles and thus detection temporarily vanished during the sequences. Figure 5 reveals the images taken during the particle tracking in the IR images. The approach responded well on the subjects during the laboratory simulated radiological exam and the hot spots were correctly tracked during the thermal video sequences. This represents the efficiency of the approach in tracking of the thermal changes within the actual situation.

6. Discussion

The proposed study presented a short review for the investigation regarding the possible overheating which occurs in the radiology examination particularly in smaller body patients or those having any external risk (e.g. tattoo). In general, radiological machines are safely made for medical scanning. However, the malfunctioning or possible mistakes in their adjustment (i.e. problem for setting the parameters of the machines such as SAR) may create the aforemen-

tioned problems. The application of thermal analysis and imaging along with machine learning provided a promising system for the detection and tracking of any overheating which occurs during the test. The approach focuses on continuous and automatic detection, monitoring and tracking of the overheating and the core temperature fluctuations on the human body. These hot spots are the points that have a high possibility for burning and physiologically have a higher possibility to be burned which represents the higher temperature regions which must be tracked and monitored during the examination to prevent potential burning. The previous relevant approach [86] gave a valuable particle filter tracking paradigm to select pixels having a high temperature for a moving object. Here an automatic clustering technique provided a thermal selection and tracking using a particle filter. The difference between these approaches is related to the moving subject and unpredictable hot spots during the radiology. It is noticeable that the approach has the ability to track the unpredictable hot spots in the moving subjects but considering the definition of the project seems unnecessary. However, it provides a significant robustness against motion artifacts that occur during the exam. This is due to a powerful clustering technique for segmenting the ROI in thermal video streams (in each frame per second). The approach considered that each pixel of the thermal image during a thermographical measurement provides the approximated temperature of the body surface. There is an approximation regarding the atmospheric transmittance between the camera and the subject which can be estimated by using the blackbody in the experiment (or controllable known thermal spots in the real situation). Though, this estimation is an approximation of the real transmittance of the atmosphere that is related to the distance of the thermal camera and the subject hot spot points (and many other neglected parameters that can be considered). Moreover, the emissivity of the targeted fabric is also another factor of this estimation. The proposed approach gave the possibility of the tracking hot spots unrelated to the actual temperature which is a function of the temperature scale. The approximation of the hot spots to provide the initialization and control points which lie under the boundary of ROI as the

temperature measured in the frame gives the possibility to track the hot area on entire video stream.

7. Conclusion

The presented approach addressed a review on the overheating which occurs during radiological examinations such as MRI and a series of thermal experiments to find the thermal suitable fabric would can be used as a radiological gown. An automatic system for the detection and tracking of the thermal fluctuations has been proposed as well. It applied HSV based kernelled k-means clustering which initialized and controlled the points which lie on the ROI boundary. Afterwards, a particle filter tracked the targeted ROI during the video sequence. The proposed approach has been tested during some experiments which closely resemble real radiology examination. Six subjects voluntarily participated on these experiments. To simulate the hot spots occurring during the radiology a controllable heating source was used near the subjects body. The results indicated promising accuracy for the proposed approach for tracking of the hot spots. However, some approximations were used regarding the neglected atmospheric transmittance of the fabric emissivity because of the independency of the proposed approach for these parameters. The approach can continuously and correctly track the heating spots. It provided substantial robustness related to the motion artifacts which occur during the medical radiology. Future work will involve more experiments to provide more concrete outcome to increase the confidence regarding the method for real examinations. Other topics which will be addressed include the estimation of the overheating even for the parts which are not in the FOV of thermal camera or internal burning which also requires further research.

8. Acknowledgment

The authors would like to thank Annette Schwerdtfeger from the Department of Electrical and Computer Engineering at Laval University for her constructive

comments and help. Also we acknowledge the help of Julien Fleuret, Seyed Alireza Ghaffari, Simon Fréchet, Félix Labrie Larrive, Marcelo Sung Ma Jo, researchers in the department of electrical and computer engineering at University Laval. This research project was conducted under the Chaire de recherche du Canada en vision infrarouge multipolaire (MIVIM).

References

[1] B. F. Jones, A reappraisal of the use of infrared thermal image analysis in medicine, IEEE transactions on medical imaging 17 (6) (1998) 1019–1027.

[2] W. C. Amalu, Nondestructive testing of the human breast: the validity of dynamic stress testing in medical infrared breast imaging, in: Engineering in Medicine and Biology Society, 2004. IEMBS'04. 26th Annual International Conference of the IEEE, Vol. 1, IEEE, 2004, pp. 1174–1177.

[3] E.-K. Ng, S. Fok, Y. Peh, F. Ng, L. Sim, Computerized detection of breast cancer with artificial intelligence and thermograms, Journal of medical engineering & technology 26 (4) (2002) 152–157.

[4] K. Parsi, S. Kossard, Thermosensitive lichen amyloidosis, International journal of dermatology 43 (12) (2004) 925–928.

[5] A. McDougali, D. Salter, Thermography of the nose and ear in relation to the skin lesions of lepromatous leprosy, tuberculosis, leishmaniasis, and lupus pernio, Journal of Investigative Dermatology 68 (1) (1977) 16–22.

[6] M. Camenzind, M. Weder, R. Rossi, C. Kowtsch, Remote sensing infrared thermography for mass-screening at airports and public events: Study to evaluate the mobile use of infrared cameras to identify persons with elevated body temperature and their use for mass screening, Tech. rep., Technical Report 204991, EMPA Materials Science and Technology (2006).

[7] M.-F. Chiang, P.-W. Lin, L.-F. Lin, H.-Y. Chiou, C.-W. Chien, S.-F. Chu, W.-T. Chiu, Mass screening of suspected febrile patients with remote-

sensing infrared thermography: alarm temperature and optimal distance, Journal of the Formosan Medical Association 107 (12) (2008) 937–944.

[8] N. Tabatabaei, A. Mandelis, B. T. Amaechi, Thermophotonic lock-in imaging of early demineralized and carious lesions in human teeth, Journal of biomedical optics 16 (7) (2011) 071402–071402.

[9] L. Zhang, A. S. Kim, J. S. Ridge, L. Y. Nelson, J. H. Berg, E. J. Seibel, Trimodal detection of early childhood caries using laser light scanning and fluorescence spectroscopy: clinical prototype, Journal of biomedical optics 18 (11) (2013) 111412–111412.

[10] D. Shastri, A. Merla, P. Tsiamyrtzis, I. Pavlidis, Imaging facial signs of neurophysiological responses, IEEE Transactions on Biomedical Engineering 56 (2) (2009) 477–484.

[11] W. G. Guntheroth, P. S. Spiers, Thermal stress in sudden infant death: is there an ambiguity with the rebreathing hypothesis?, Pediatrics 107 (4) (2001) 693–698.

[12] M. Russell, R. Vink, Increased facial temperature as an early warning in sudden infant death syndrome, Medical hypotheses 57 (1) (2001) 61–63.

[13] S. Sunderam, I. Osorio, Mesial temporal lobe seizures may activate thermoregulatory mechanisms in humans: an infrared study of facial temperature, Epilepsy & Behavior 4 (4) (2003) 399–406.

[14] D. Shastri, A. Merla, P. Tsiamyrtzis, I. Pavlidis, Imaging facial signs of neurophysiological responses, IEEE Transactions on Biomedical Engineering 56 (2) (2009) 477–484.

[15] A. Merla, P. A. Mattei, L. Di Donato, G. L. Romani, Thermal imaging of cutaneous temperature modifications in runners during graded exercise, Annals of biomedical engineering 38 (1) (2010) 158–163.

[16] G.-A. Bilodeau, A. Torabi, M. Lévesque, C. Ouellet, J. P. Langlois, P. Lema, L. Carmant, Body temperature estimation of a moving subject from thermographic images, Machine Vision and Applications 23 (2) (2012) 299–311.

[17] B. Yousefi, J. Fleuret, S. A. Ghaffari, S. Fréchet, F. L. Larrivée, M. S. M. Jo, M. Klein, X. Maldague, R. Watts, Unsupervised automatic tracking of thermal changes in human body, Advanced Infrared Technology & Applications (2015) 152.

[18] medicine, `http://www.medicinenet.com/mri_scan/page2.htm`, accessed: March, 2014.

[19] Effects of mri, `http://www.mri-side-effects.com/mri_skin_swelling`, accessed: March, 2014.

[20] E. G. Eising, J. Hughes, F. Nolte, W. Jentzen, A. Bockisch, Burn injury by nuclear magnetic resonance imaging, Clinical imaging 34 (4) (2010) 293–297.

[21] E. Picano, Sustainability of medical imaging, Bmj 328 (7439) (2004) 578–580.

[22] S. Simi, M. Ballardin, M. Casella, D. De Marchi, V. Hartwig, G. Giovannetti, N. Vanello, S. Gabbriellini, L. Landini, M. Lombardi, Is the genotoxic effect of magnetic resonance negligible? low persistence of micronucleus frequency in lymphocytes of individuals after cardiac scan, Mutation Research/Fundamental and Molecular Mechanisms of Mutagenesis 645 (1) (2008) 39–43.

[23] S. Bonassi, A. Znaor, M. Ceppi, C. Lando, W. P. Chang, N. Holland, M. Kirsch-Volders, E. Zeiger, S. Ban, R. Barale, et al., An increased micronucleus frequency in peripheral blood lymphocytes predicts the risk of cancer in humans, Carcinogenesis 28 (3) (2006) 625–631.

[24] V. Hartwig, G. Giovannetti, N. Vanello, M. Lombardi, L. Landini, S. Simi, Biological effects and safety in magnetic resonance imaging: a review, International journal of environmental research and public health 6 (6) (2009) 1778–1798.

[25] M. F. Dempsey, B. Condon, D. M. Hadley, Investigation of the factors responsible for burns during mri, Journal of Magnetic Resonance Imaging 13 (4) (2001) 627–631.

[26] E. problem reporting system, Hazard-thermal injuries and patient monitoring during mri studies, Tech. rep., Health Devices (1991).

[27] F. G. Shellock, E. Kanal, Burns associated with the use of monitoring equipment during mr procedures, Journal of Magnetic Resonance Imaging 6 (1) (1996) 271–272.

[28] E. Kanal, F. Shellock, Burns associated with clinical mr examinations., Radiology 175 (2) (1990) 585.

[29] T. Brown, B. Goldstein, J. Little, Severe burns resulting from magnetic resonance imaging with cardiopulmonary monitoring. risks and relevant safety precautions., American journal of physical medicine & rehabilitation/Association of Academic Physiatrists 72 (3) (1993) 166–167.

[30] G. Bashein, G. SYROVY, Burns associated with pulse oximetry during magnetic resonance imaging, The Journal of the American Society of Anesthesiologists 75 (2) (1991) 382–382.

[31] S. C. HALL, G. Stevenson, S. SURESH, Burn associated with temperature monitoring during magnetic resonance imaging, The Journal of the American Society of Anesthesiologists 76 (1) (1992) 152–152.

[32] S. Jones, W. Jaffe, R. Alvi, Burns associated with electrocardiographic monitoring during magnetic resonance imaging, Burns 22 (5) (1996) 420–421.

[33] S. Keens, A. Laurence, Burns caused by ecg monitoring during mri imaging, Anaesthesia 51 (12) (1996) 1188–1189.

[34] P. Levallois, Hypersensitivity of human subjects to environmental electric and magnetic field exposure: a review of the literature., Environmental health perspectives 110 (Suppl 4) (2002) 613.

[35] I. Guideline, Guidelines for limiting exposure to time-varying electric, magnetic, and electromagnetic fields (up to 300 ghz), Health Phys 74 (4) (1998) 494–522.

[36] A. Ahlbom, J. Bridges, W. De Jong, T. Jung, O. Mattsson, J.-m. Pagès, K. Rydzynski, D. Stahl, M. Thomsen, Scientific committee on emerging and newly identified health risks scenihr risk assessment of products of nanotechnologies.

[37] D. W. McRobbie, E. A. Moore, M. J. Graves, M. R. Prince, MRI from Picture to Proton, Cambridge university press, 2007.

[38] D. McNeil, Mris strong magnets cited in accidents, New York Times 19 (2005) 2005.

[39] U.s. food and drug administration (fda) medical device reporting (mdr), `http://www.fda.gov`, accessed: May 4, 2009.

[40] Ecri health device alerts (hda), `http://www.mdsr.ecri.org/`, accessed: May 4, 2009.

[41] F. G. Shellock, Radiofrequency energy-induced heating during mr procedures: a review, Journal of Magnetic Resonance Imaging 12 (1) (2000) 30–36.

[42] F. G. Shellock, Magnetic resonance safety update 2002: implants and devices, Journal of magnetic resonance imaging 16 (5) (2002) 485–496.

[43] D. Formica, S. Silvestri, Biological effects of exposure to magnetic resonance imaging: an overview, Biomedical engineering online 3 (1) (2004) 1.

[44] F. Krasin, H. Wagner, Biological effects of nonionizing electromagnetic radiation, Encyclopedia of Medical Devices and Instrumentation.

[45] F. G. Shellock, B. Rothman, D. Sarti, Heating of the scrotum by high-field-strength mr imaging., AJR. American journal of roentgenology 154 (6) (1990) 1229–1232.

[46] F. Shellock, J. V. Crues, Corneal temperature changes induced by high-field-strength mr imaging with a head coil., Radiology 167 (3) (1988) 809–811.

[47] M. Vahlensieck, Tattoo-related cutaneous inflammation (burn grade i) in a mid-field mr scanner, European radiology 10 (1) (2000) 197–197.

[48] W. A. Wagle, M. Smith, Tattoo-induced skin burn during mr imaging, American Journal of Roentgenology.

[49] M. Kreidstein, D. Giguere, A. Freiberg, Mri interaction with tattoo pigments: case report, pathophysiology, and management., Plastic and reconstructive surgery 99 (6) (1997) 1717–1720.

[50] Particular requirements for basic safety and essential performance of magnetic resonance equipment for medical diagnosis, International Electrotechnical Commission IEC (2002) 60601-2-33 2nd ed.; International Electrotechnical Commission: Geneva, Switzerland (2002) 33.

[51] E. R. Adair, L. G. Berglund, On the thermoregulatory consequences of nmr imaging, Magnetic resonance imaging 4 (4) (1986) 321–333.

[52] F. G. Shellock, D. J. Schaefer, J. V. Crues, Alterations in body and skin temperatures caused by magnetic resonance imaging: is the recommended exposure for radiofrequency radiation too conservative?, The British journal of radiology 62 (742) (1989) 904–909.

[53] C. A. Van den Berg, B. Van den Bergen, J. B. Van de Kamer, B. W. Raaymakers, H. Kroeze, L. W. Bartels, J. J. Lagendijk, Simultaneous b

1+ homogenization and specific absorption rate hotspot suppression using a magnetic resonance phased array transmit coil, Magnetic resonance in medicine 57 (3) (2007) 577–586.

[54] F. Liu, H. Zhao, S. Crozier, Calculation of electric fields induced by body and head motion in high-field mri, Journal of Magnetic Resonance 161 (1) (2003) 99–107.

[55] M. L. Meltz, Radiofrequency exposure and mammalian cell toxicity, genotoxicity, and transformation, Bioelectromagnetics 24 (S6) (2003) S196–S213.

[56] E. Diem, C. Schwarz, F. Adlkofer, O. Jahn, H. Rüdiger, Non-thermal dna breakage by mobile-phone radiation (1800mhz) in human fibroblasts and in transformed gfsh-r17 rat granulosa cells in vitro, Mutation Research/Genetic Toxicology and Environmental Mutagenesis 583 (2) (2005) 178–183.

[57] T. Nikolova, J. Czyz, A. Rolletschek, P. Blyszczuk, J. Fuchs, G. Jovtchev, J. Schuderer, N. Kuster, A. M. Wobus, Electromagnetic fields affect transcript levels of apoptosis-related genes in embryonic stem cell-derived neural progenitor cells, The FASEB journal 19 (12) (2005) 1686–1688.

[58] M. R. Scarfì, A. M. Fresegna, P. Villani, R. Pinto, C. Marino, M. Sarti, P. Altavista, A. Sannino, G. A. Lovisolo, Exposure to radiofrequency radiation (900 mhz, gsm signal) does not affect micronucleus frequency and cell proliferation in human peripheral blood lymphocytes: an interlaboratory study, Radiation research 165 (6) (2006) 655–663.

[59] R. Saunders, C. Kowalczuk, C. Beechey, R. Dunford, Studies of the induction of dominant lethals and translocations in male mice after chronic exposure to microwave radiation, International Journal of Radiation Biology 53 (6) (1988) 983–992.

[60] A. Kangarlu, R. Burgess, H. Zhu, T. Nakayama, R. Hamlin, A. Abduljalil, P. Robitaille, Cognitive, cardiac, and physiological safety studies in ultra high field magnetic resonance imaging, Magnetic resonance imaging 17 (10) (1999) 1407–1416.

[61] S. J. Regel, S. Negovetic, M. Röösli, V. Berdiñas, J. Schuderer, A. Huss, U. Lott, N. Kuster, P. Achermann, Umts base station-like exposure, well-being, and cognitive performance, Environmental health perspectives (2006) 1270–1275.

[62] D. Schaefer, B. Barber, C. Gordon, J. Zielonka, J. Hecker, Thermal effects of magnetic resonance imaging, Book of abstracts, Society for magnetic resonance in medicine Volume 2.

[63] F. Shellock, D. Schaefer, J. Crues, Evaluation of skin blood flow, body and skin temperatures in man during mr imaging at high levels of rf energy, Magn Reson Imaging 7 (Suppl 1) (1989) 335.

[64] D. K. Kido, T. W. Morris, J. L. Erickson, D. B. Plewes, J. H. Simon, Physiologic changes during high field strength mr imaging, American journal of neuroradiology 8 (2) (1987) 263–266.

[65] F. G. Shellock, D. J. Schaefer, E. Kanal, Physiologic responses to an mr imaging procedure performed at a specific absorption rate of 6.0 w/kg., Radiology 192 (3) (1994) 865–868.

[66] D. J. Schutt, M. M. Swindle, K. L. Helke, G. Bastarrika, F. Schwarz, D. Haemmerich, Sequential activation of ground pads reduces skin heating during radiofrequency tumor ablation: in vivo porcine results, IEEE Transactions on Biomedical Engineering 57 (3) (2010) 746–753.

[67] F. Ibrahim, M. Barbic, C. Druzgalski, Stripe sensor tomography and application to microcoil magnetic resonance imaging, 2009.

[68] D. J. Schutt, M. M. Swindle, K. L. Helke, G. Bastarrika, F. Schwarz, D. Haemmerich, Sequential activation of ground pads reduces skin heat-

ing during radiofrequency tumor ablation: in vivo porcine results, IEEE Transactions on Biomedical Engineering 57 (3) (2010) 746–753.

[69] R. Das, H. Yoo, Innovative design of implanted medical lead to reduce mri-induced scattered electric fields, Electronics Letters 49 (5) (2013) 323–324.

[70] J. C. Gayton, P. Sensiba, B. F. Imbrogno, I. Venkatarayappa, J. Tsatalis, M. J. Prayson, The effects of magnetic resonance imaging on surgical staples: an experimental analysis, Journal of Trauma and Acute Care Surgery 70 (5) (2011) 1279–1281.

[71] M. Manabe, H. Yamazaki, K. Sakai, Shape factor simulation for the thermal radiation environment of the human body and the vrml visualization, Building and environment 39 (8) (2004) 927–937.

[72] E. Badel, C. Delisee, J. Lux, 3d structural characterisation, deformation measurements and assessment of low-density wood fibreboard under compression: The use of x-ray microtomography, Composites Science and Technology 68 (7) (2008) 1654–1663.

[73] S. Jaganathan, H. V. Tafreshi, B. Pourdeyhimi, Modeling liquid porosimetry in modeled and imaged 3-d fibrous microstructures, Journal of colloid and interface science 326 (1) (2008) 166–175.

[74] V. S. Cheng, J. Bai, Y. Chen, A high-resolution three-dimensional far-infrared thermal and true-color imaging system for medical applications, Medical engineering & physics 31 (9) (2009) 1173–1181.

[75] R. Sharma, B. R. Locke, Jet fuel toxicity: skin damage measured by 900-mhz mri skin microscopy and visualization by 3d mr image processing, Magnetic resonance imaging 28 (7) (2010) 1030–1048.

[76] P. Markelj, D. Tomaževič, B. Likar, F. Pernuš, A review of 3d/2d registration methods for image-guided interventions, Medical image analysis 16 (3) (2012) 642–661.

[77] S. Lagüela, J. Armesto, P. Arias, J. Herráez, Automation of thermographic 3d modelling through image fusion and image matching techniques, Automation in Construction 27 (2012) 24–31.

[78] S. Vidas, P. Moghadam, Heatwave: A handheld 3d thermography system for energy auditing, Energy and buildings 66 (2013) 445–460.

[79] C. Siewert, S. Dänicke, S. Kersten, B. Brosig, D. Rohweder, M. Beyerbach, H. Seifert, Difference method for analysing infrared images in pigs with elevated body temperatures, Zeitschrift für Medizinische Physik 24 (1) (2014) 6–15.

[80] P. Yousefi, A. H. Jalab, W. R. Ibrahim, N. F. M. Noor, M. N. Ayub, G. Abdullah, Water-body segmentation in satellite imagery applying modified kernel k-means selection, Malaysian Journal of Computer Science.

[81] M. Isard, A. Blake, Condensationconditional density propagation for visual tracking, International journal of computer vision 29 (1) (1998) 5–28.

[82] F. Zhang, E. R. Hancock, C. Goodlett, G. Gerig, Probabilistic white matter fiber tracking using particle filtering and von mises–fisher sampling, Medical image analysis 13 (1) (2009) 5–18.

[83] I. Smal, E. Meijering, K. Draegestein, N. Galjart, I. Grigoriev, A. Akhmanova, M. Van Royen, A. B. Houtsmuller, W. Niessen, Multiple object tracking in molecular bioimaging by rao-blackwellized marginal particle filtering, Medical Image Analysis 12 (6) (2008) 764–777.

[84] I. Smal, E. Meijering, Quantitative comparison of multiframe data association techniques for particle tracking in time-lapse fluorescence microscopy, Medical image analysis 24 (1) (2015) 163–189.

[85] C. Ohman, Practical methods for improving thermal measurements, in: Thermal Infrared Sensing Applied to Energy Conservation in Building Envelopes, International Society for Optics and Photonics, 1982, pp. 204–212.

[86] G.-A. Bilodeau, A. Torabi, M. Lévesque, C. Ouellet, J. P. Langlois, P. Lema, L. Carmant, Body temperature estimation of a moving subject from thermographic images, Machine Vision and Applications 23 (2) (2012) 299–311.